

Giant interference line shift in absorption from a split ground state

M. S. Zubova and V. P. Kochanov

Institute of Atmospheric Optics, Siberian Branch, Russian Academy of Sciences

(Submitted 25 November 1991; resubmitted 28 January 1992)

Zh. Eksp. Teor. Fiz. **101**, 1772–1786 (June 1992)

Nonlinear interference phenomena in closed Λ - and V -type systems are examined analytically and by means of numerical calculations. It is shown that in a Λ -type system, i.e., one with a split ground state, the stationary-absorption line profile (fluorescence excitation spectrum) is shifted and broadened by a resonance radiation field. As the magnitude of the splitting decreases, the interference shift and interference broadening increase to limiting values which are determined by the degree of radiation coherence, time of flight of the atoms through the atomic beam, and collisional relaxation, and can amount to > 1000 linewidths of optical transitions. In the presence of collisions, the line profile exhibits narrowing as the pressure increases.

1. INTRODUCTION

The article of Ref. 1 and the literature cited there showed that in a closed three-level system whose lowest level is the ground level and whose intermediate level is metastable, the absorption spectra of pulsed resonance radiation and stimulated fluorescence contain, valleys and peaks which in nonlinear spectroscopy are unusual within a homogeneously broadened line. The formation of such structures is due to redistribution of the populations of the levels in the course of the combined action of the field and of spontaneous decay, which result in bleaching of the medium.

Generalization of the treatment given in Ref. 1 to the case in which the ground and metastable levels are close makes it necessary to take into account nonlinear interference effects (NIE) along with population effects.² NIE arise because the radiation acting on the quantum system induces polarization in forbidden low-frequency or optical transitions, and because the latter couple the polarizations of allowed optical transitions on which absorption takes place and the observed line profile is formed. NIE in systems with three or more levels are known in double-resonance laser spectroscopy^{3–5} and produce a number of nontrivial spectroscopic manifestations.^{6–12} In most cases, these manifestations were studied on excited atomic states, i.e., open systems, with the use of two laser fields resonant with allowed transitions having a common level.

The distinguishing features of the system under discussion, which, when the two lower levels are close together, can be treated as a resonance transition from a split ground state, are that the effect can build up because of closure, thus allowing NIE to occur in nonsaturating fields, as well as the extremely low probability of radiative transitions between the components of the splitting.¹¹ The latter fact predetermines, in particular, the existence of superpositions of states such that population of the upper level by the resonance field and correspondingly, induced fluorescence do not occur. This was observed in experiments with excitation of sodium vapor by the radiation of a multimode dye laser as a sharp drop in fluorescence intensity in a narrow range of values of the magnetic field causing rearrangement of the sublevels of the ground state.^{10,11} Its interpretation is given in Ref. 12 in terms of coherent “nonabsorbing states” by means of a three-level diagram with widely spaced lower levels and two optical fields resonant with the optical transitions.

A previously unmentioned possible manifestation of

NIE under stationary absorption conditions during the transition from the split ground state of a closed three-level system is the formation of appreciable interference shifts and line broadening.

The mechanism for their formation can be clarified by drawing an analogy between NIE and the well studied spectral exchange or line interference.^{14–17} The existence of the analogy follows from the presence, in both cases, of coupling of the polarizations of allowed transitions. For spectral exchange, this coupling (cross-relaxation) arises from collisions, and is independent of radiation intensity over a wide range. For the interference effect, on the other hand, it takes place due to the simultaneous action of the field on allowed transitions through the induced polarizations of forbidden transitions, and is maximal in the absence of collisions. In both cases, the effective coupling parameters contain real and imaginary parts. From this, one should expect a similarity of the characteristic manifestations of spectral exchange and NIE in the form of an additional shift and broadening (or narrowing) of the lines and collapse of coupled lines as the cross-relaxation parameters increase. At the same time, the difference in the physical nature of these parameters radically affects the nature of these manifestations. Specifically, in the case of the interference effect, because of the very short response time of the polarization on a forbidden transition, the coupling parameter increases almost indefinitely as the splitting of the ground state decreases. There will be a corresponding increase of the shift and broadening of the line formed as a result of the collapse. Since under stationary conditions the latter is known to complete because of the closure of the system and its long interaction time with the field, the limitations on the width and shift can arise only from collisions, from the nonmonochromaticity of the radiation, and from the escape of the atoms from the light beam.

The present article is devoted to a theoretical description and estimation of the attainable values of this shift, as well as an analysis of its behavior as a function of the magnitude of the splitting, field intensity, and relaxation parameters of the system in the absence and presence of collisions.

2. STATEMENT OF THE PROBLEM

The system, consisting of the ground (0), excited (1) and metastable (2) levels, and interacting simultaneously with the 1–0 and 1–2 transitions of an optical radiation field,

will be described by the standard equations for the density matrix in a model of relaxation constants and homogeneous broadening. In the interaction representation and rotating wave approximation, these equations are

$$\begin{aligned}
\dot{R}_1 + (\Gamma - i\Omega)R_1 &= iV_1(\rho_0 - \rho_1) + iV_2R_3, \\
\dot{R}_2 + [\Gamma_2 - i(\Omega + \Delta)]R_2 &= iV_2(\rho_2 - \rho_1) + iV_1R_3^*, \\
\dot{R}_3 + (\Gamma_3 + i\Delta)R_3 &= iV_2R_1 - iV_1R_2^*, \\
\dot{\rho}_0 - A_1\rho_1 + \gamma(\rho_0 - \rho_2) &= 2V_1 \operatorname{Re} iR_1, \\
\dot{\rho}_2 - A_2\rho_1 - \gamma(\rho_0 - \rho_2) &= 2V_2 \operatorname{Re} iR_2, \\
\rho_0 + \rho_1 + \rho_2 &= 1,
\end{aligned} \tag{1}$$

where ρ_i ($i = 0, 1, 2$) are the level populations, R_i and Γ_i ($i = 1, 2, 3$), respectively, are the slowly changing parts of the nondiagonal elements of the density (polarization) matrix and the relaxation constants of the 1-0, 1-2, and 2-0 transitions, $V_i = V_i^* = d_i E / 2\hbar$ is the (generally time-dependent) amplitude envelope of the electric field of the light wave, d_i and A_i ($i = 1, 2$) are respectively, the matrix elements of the dipole moment and the first Einstein coefficients of the 1-0 and 1-2 allowed optical transitions, γ is the rate of collisional transfer of excitation from level 2 to level 0 and vice versa, $\Omega = \omega - \omega_{10}$ is the detuning of the laser radiation frequency ω from the frequency ω_{10} of the 1-0 transition, and $\Delta = \omega_{20}$ is the frequency of the 2-0 forbidden low-frequency transition or the magnitude of the ground-state splitting.

Omitted from the first three equations of the system (1) are the terms responsible for the collisional displacement of the lines; these terms may be neglected in an examination of the qualitative behavior of the interference shift.

Equations (1) are an extension of the equations used in Ref. 1 in the discussion of a three-level system with widely spaced levels 0 and 2. The system (1) additionally contains an equation for the polarization R_3 induced by a field on the optically forbidden transition 2-0. As is evident from Eq. (1), the quantity R_3 , which enters into the equations for the polarizations of allowed transitions and is itself expressed in terms of R_1 and R_2 , reflects the interference between them, which is essential for the formation of the stationary absorption line profile. This very important point will be illustrated by writing, for $\dot{R}_1 = \dot{R}_2 = \dot{R}_3 = 0$, the equations for R_1 and R_2 separately with substitution into them of the quantity R_3 from the third equation of the system (1):

$$\begin{aligned}
\left[\Gamma_1 - i\Omega + \frac{V_2^2}{\Gamma_3 + i\Delta} \right] R_1 - \frac{V_1 V_2}{\Gamma_3 + i\Delta} R_2^* &= iV_1(\rho_0 - \rho_1), \\
\left[\Gamma_2 - i(\Omega + \Delta) + \frac{V_1^2}{\Gamma_3 - i\Delta} \right] R_2 - \frac{V_1 V_2}{\Gamma_3 - i\Delta} R_1^* &= iV_2(\rho_2 - \rho_1).
\end{aligned} \tag{1'}$$

It follows from Eqs. (1') that, in contrast to collisional spectral exchange, coupling of the complex-conjugate polarizations R_1 and R_2^* takes place in this case, and the coupling parameters $V_1 V_2 / (\Gamma_3 \pm i\Delta)$ increase indefinitely in the absence of collisions ($\Gamma_3 = 0$) and as $\Delta \rightarrow 0$. The third terms in square brackets preceding R_1 and R_2 behave similarly. These characteristics of NIE in the system under consideration ultimately give rise to the large interference shifts and widths discussed.

Another manifestation of polarization on a forbidden transition is related to the dominant influence of the polarization on the dynamics of absorption over times exceeding the relaxation times of optical transitions. Indeed, using the condition, applicable to such times, for the applicability of the balance equations $\dot{R}_1 = \dot{R}_2 = 0$, and eliminating R_1 , R_2 from Eqs. (1), one can obtain closed equations of motion for a generalized two-level system¹⁸ consisting of levels 0 and 2, where the polarization R_3 describes two-quantum transitions between them via the excited level 1. This approximation holds for $\rho_1 \ll 1$, which is the case, for example, if $\Omega \gtrsim \gamma_1$.

Note that the above system of equations corresponds to three experimental arrangements. First, as was done in the description (1), the resonance field used can be radiation with arbitrary polarization and carrier frequency $\omega \approx \omega_{10}$, ω_{12} , interacting with transitions whose lower levels are components of the fine or hyperfine atomic structure. The magnitudes of A_1 and A_2 are generally different, and because $A_1 \propto d_1^2 \omega_{10}^3$, $A_2 \propto d_2^2 \omega_{12}^3$ (see, for example, Ref. 19) and $\omega_{10} - \omega_{12} = \Delta \ll \omega_{10}, \omega_{12}$, we find that $V_1^2 / V_2^2 = A_1 / A_2$ holds to a high degree of accuracy. Second, by placing the atoms in a magnetic field, as the sublevels 0 and 2 of the split ground state we can select magnetic sublevels, weakly coupled with the others, of the same (or different) HFS components if the field E is the sum of two fields with the same frequency ω and opposite circular polarizations. Here $A_1 = A_2$ (or $A_1 \neq A_2$), the ratio of V_1 to V_2 is arbitrary, and the value of Δ can vary from zero to high values as the magnetic field changes. Finally, the field E may be assumed to consist of two components with substantially different frequencies ω_1 and ω_2 , resonant with the 1-0 and 1-2 transitions, if the quantities Ω and $\Omega + \Delta$ in the equations for R_1 and R_2 are replaced by the frequency detunings of the first and second fields from the eigenfrequencies of the corresponding resonance transitions. In this case, levels 2 and 0 should be sufficiently spaced ($\Delta \gg \Gamma_i$) so that the resonance approximation holds for each of the optical transitions separately.

The first two forms of the statement of the problem correspond to the classical level-crossing scheme, and the last variant is examined in detail in Ref. 12 in the case $A_1 = A_2$ from the standpoint of the analysis of the behavior in the shape of narrow resonances of the dependence $\rho_1(\Delta)$. We shall then examine the line profiles in the absorption and fluorescence excitation spectra for the level-crossing scheme.

As the unknown quantity in the solution of Eqs. (1), we take the population of the upper level ρ_1 , which is proportional to the intensity of the spontaneous emission from level 1 to levels 0 and 2 integrated over the spectrum, or the field energy, $\mathcal{P} = 2V_1 \operatorname{Re}(iR_1) + 2V_2 \operatorname{Re}(iR_2)$, which is proportional to the radiation absorption coefficient in the first and second forms of the statement of the problem. When the atom is acted on by continuous radiation, it follows from Eqs. (1) that in the stationary limit, the quantities ρ_1 and \mathcal{P} are related by the simple expression $\mathcal{P} = -\gamma_1 \rho_1$, where γ_1 is the rate of decay of the upper level, which in the absence of quenching collisions is equal to the reciprocal of the radiative decay time: $\gamma_1 = A_1 + A_2$. Then, using the term "line profile" for brevity, we shall use it to refer to the dependence $\rho_1(\Omega)$ or $\mathcal{P}(\Omega)$.

3. DYNAMICS OF FORMATION OF THE SPECTRA; STATIONARY ABSORPTION UNDER COLLISIONLESS CONDITIONS

We shall analyze the dynamics of line-profile formation in the absence of collisions, when the polarization interference is appreciable. We shall be primarily interested in the characteristics of the stationary profile which are determined by NIE, and in the times of its formation. In accordance with the situation in question, neglecting the radiative decay of level 2, in Eqs. (1) we assume $\gamma = \Gamma_3 = 0$, $\Gamma_1 = \Gamma_2 = \gamma_1/2$, $\gamma_1 = A_1 + A_2$.

The variety of the possible experimental arrangements discussed in Sec. 2 permits an appreciable freedom in the selection of the values of the parameters V_1, V_2 and A_1, A_2 . At first, to simplify the analysis, we shall keep these parameters constant and equal, and examine the influence exerted on the population $\rho_1(\Omega, t = \tau)$, at the instant the action of the field ends, by the pulse length τ , the magnitude of the splitting Δ , and the initial population ratio of levels 2 and 0.

The results of the numerical solution of Eqs. (1) for this case are given in Fig. 1.²⁾ It is evident from Fig. 1a, b that for relatively short pulse lengths $\tau \lesssim 40\gamma_1^{-1}$, as the laser radiation frequency ω is being adjusted, two profiles are formed whose centers are located at eigenfrequencies ω_{10} and ω_{12} of the allowed transitions, and inside each of these profiles are dips of nonstationary saturated absorption, caused by bleaching of the medium due to the population effect.¹ In this situation, however, in contrast to Ref. 1, as $\tau \rightarrow \infty$, no bleaching of the medium takes place, as should be the case in the absence of radiative transitions from the metastable level to the ground level without the influence of interference. Thus, the most obvious role of NIE is in forming a single line profile instead of two separate ones, with the population effect dominating in the process. In other words, the field-induced coupling of optical transitions through the forbidden transition leads to the confluence (collapse) of the stationary absorption lines on these transitions. Owing to the closure of the system, the collapse takes place at any values of the field amplitudes and spacing of the lower levels and is complete. As is evident from Fig. 1, as Δ increases, the maximum amplitude of the stationary profile formed decreases, and the profile is broadened. Obviously, at sufficiently large Δ , NIE and stationary absorption become insignificant, and the situation is reduced to that discussed in Ref. 1.

The position of the line center Ω_0 in the case $V_1 = V_2$ and $A_1 = A_2$ is determined only by the magnitude of the splitting: $\Omega_0 = -\Delta/2$. As is evident from a comparison of Fig. 1a, b and Fig. 1c, the inequality of the initial populations of levels 2 and 0 creates an asymmetry of the nonstationary profiles with respect to Ω_0 .

An increase in the ratio of the magnitudes of interaction of the 1-2 and 1-0 transitions with the field V_2/V_1 in the case $A_1 \neq A_2$ leads to an increase in the amplitude of the peak of the excitation spectrum of stationary fluorescence, in contrast to the behavior of the maxima of the nonstationary profiles, which remain practically unchanged in size (Fig. 2). Moreover, as a result of the special selection of $\Delta = \gamma_1$ and $V_2^2/V_1^2 \ll 1$, the centers of the profiles on the scale of the figure are indistinguishable from ω_{10} ($\Omega = 0$). Varying Δ while maintaining $V_2^2 \ll V_1^2$ gives an appreciable shift of the

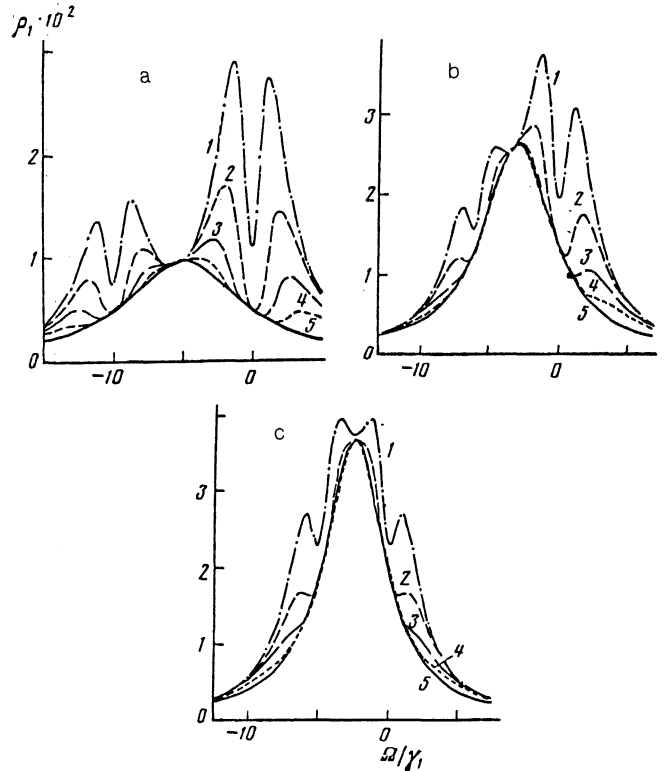


FIG. 1. Fluorescence excitation spectrum after cessation of a rectangular pulse of length τ with $A_1 = A_2 = V_1 = V_2 = 0.5\gamma_1$; $\tau\gamma_1 = 20$ (1), 40 (2), 80 (3), 160 (4), ∞ (5); $\Delta = 10\gamma_1$ (a), $6\gamma_1$ (b), $5\gamma_1$ (c); $\rho_0(0) = 0.7$, $\rho_2(0) = 0.3$ (a,b); $\rho_0(0) = \rho_2(0) = 0.5$ (c); $\gamma = \Gamma_3 = 0$, $\Gamma_1 = \Gamma_2 = \gamma_1/2$.

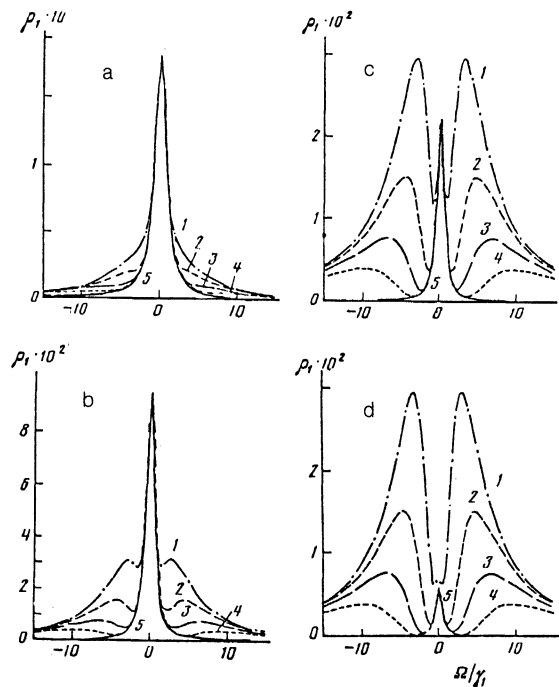


FIG. 2. Population $\rho_1(\Omega, \tau)$ of the upper level after cessation of the pulse for $A_1 = 0.4\gamma_1$, $A_2 = 0.6\gamma_1$, $\Delta = V_1 = \gamma_1$ as a function of the magnitude of V_2 : $V_2 = 0.3\gamma_1$ (a), $0.15\gamma_1$ (b), $0.06\gamma_1$ (c), $0.03\gamma_1$ (d); $\tau\gamma_1 = 20$ (1), 40 (2), 60 (3), 80 (4), ∞ (5); $\rho_0(0) = 1$; $\gamma = \Gamma_3 = 0$, $\Gamma_1 = \Gamma_2 = \gamma_1/2$.

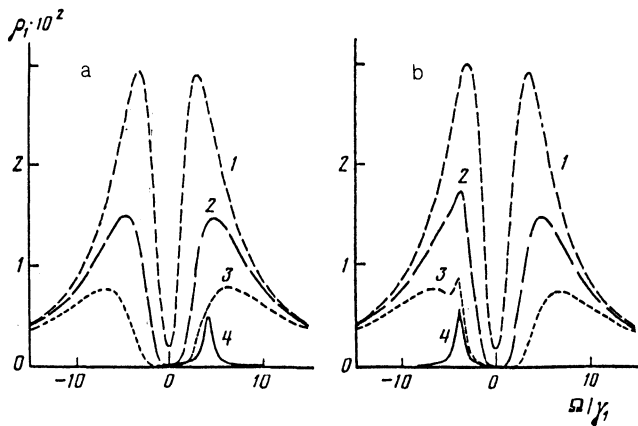


FIG. 3. Displacement of the excitation spectrum of stationary fluorescence with respect to nonstationary spectra for $\Delta = 0.24 \gamma_1$ (a) and $\Delta = 4.24 \gamma_1$ (b). $V_2 = 0.03 \gamma_1$; $\tau\gamma_1 = 20$ (1), 40 (2), 80 (3), ∞ (4). The values of the remaining parameters are the same as in Fig. 2.

stationary line relative to the centers of the non-stationary ones, both to the right and to the left of ω_{10} (Fig. 3). The existence of such a shift was discussed qualitatively in the Introduction. Its formation is a second, and generally speaking, less obvious consequence of the interference effect in a three-level system.

We shall discuss this shift quantitatively. The exact solution of Eqs. (1) for $\gamma = \Gamma_3 = 0$ in the stationary limit is

$$\begin{aligned} \rho_1 &= (\gamma_1 V_1^2 V_2^2 / B) / [(\Omega - \Omega_0)^2 + \Gamma^2], \\ \Omega_0 B &= -\Delta A_2 V_1^2 + (A_2 V_1^4 - A_1 V_2^4) / \Delta, \\ \Gamma^2 &= \gamma_1^2 / 4 + V_1^2 V_2^2 \{ \Delta^2 A_1 A_2 + 2A_1^2 V_2^2 + 2A_2^2 V_1^2 \\ &+ [2\gamma_1 (A_1 V_2^4 + A_2 V_1^4) + (\gamma_1^2 + 4A_1 A_2) V_1^2 V_2^2] / \Delta^2 \} / B^2, \\ B &= A_1 V_2^2 + A_2 V_1^2. \end{aligned} \quad (2)$$

It follows from (2) that when $\Delta \rightarrow 0$, the quantities $|\Omega_0|$ and Γ increase indefinitely, and the sign of Ω_0 is determined by the relation between the quantities A_1 , A_2 , V_1 , V_2 , and Δ and can change with the magnitude of the splitting and with the field intensity. These characteristics of the solution are seen most distinctly in the first two versions of the experimental arrangement, when the expressions (2) are simplified:

$$\begin{aligned} \text{a) } A_2 / A_1 &= V_2^2 / V_1^2 = q: \\ \rho_1 &= 1/2 (1+q) V_1^2 / [(\Omega - \Omega_0)^2 + \Gamma^2], \\ \Omega_0 &= -1/2 \Delta + 1/2 (1-q) V_1^2 / \Delta, \\ \Gamma^2 &= 1/4 \gamma_1^2 + 1/4 \Delta^2 + 1/2 (1+q) V_1^2 + 1/4 (1+10/3 q + q^2) V_1^4 / \Delta^2, \quad (2a) \\ \text{b) } A_1 &= A_2: \\ \rho_1 &= [2q / (1+q)] V_1^2 / [(\Omega - \Omega_0)^2 + \Gamma^2], \quad (2b) \\ \Omega_0 &= -\Delta / (1+q) + (1-q) V_1^2 / \Delta, \\ \Gamma^2 &= 1/4 \gamma_1^2 + \Delta^2 q / (1+q)^2 + 2q V_1^2 / (1+q) + 4q V_1^4 / \Delta^2. \end{aligned}$$

Equations (2a) and (2b) fully explain the behavior of the stationary fluorescence excitation spectrum, shown in Figs. 1–3. From them it is evident that the interference shift is proportional to the field intensity and as V_1 increases and/or Δ decreases, it takes place in the direction of shorter wavelengths for $q < 1$ [i.e., $A_2 < A_1$ in case (a) and $V_2 < V_1$ in case (b)], and in the direction of longer wavelengths for $q > 1$. For $q = 1$, the center of the stationary profile is in the middle

of the frequencies of the allowed transition. In the limit $V_1 \rightarrow 0$, the NIE induced last terms in the expressions for Ω_0 and Γ^2 (2a), (2b) disappear. At the same time, the halfwidth Γ contains a field-independent addition to the natural halfwidth $\gamma_1/2$, related to the splitting Δ . The third terms in the expressions (2a) for Γ^2 describe an ordinary field line broadening.²⁰

The fact that $|\Omega_0|$ and Γ approach ∞ as $\Delta \rightarrow 0$ is a consequence of the practical absence of a time lag of the coherence induced by the radiation on the low-frequency forbidden transition in the absence of collisions. The actual magnitude of the shift and broadening under the conditions in question can be limited only by the nonmonochromaticity of the light, neglected in Eqs. (1), and transit effects. Indeed, since the initial equations (1) are valid for time intervals shorter than the radiation coherence time of real lasers and shorter than the transit of atoms through the light beam, for the effect to exist, it is necessary that a stationary spectrum be able to form completely in that time.

A definite idea of this process can be obtained from Figs. 1–3, and a more complete picture of the dynamics of the formation of the spectrum is given by Fig. 4. The appreciable structure of the spectrum at small τ (Fig. 4a) is due to NIE and is formally explained by the fairly high (eighth) order of the characteristic equation of the system (1). The solutions of this equation contain complex roots associated with various combinations of the polarizations R_1 , R_2 , R_3 ; this gives several scales of Rabi oscillations in time and over the spectrum. Small oscillations of ρ_1 at large τ are caused by oscillations of R_3 as the least time-lagged component of the line profile. Figure 4a also clearly reflects the absence of absorption, described in Ref. 1, in the form of a decrease to zero in the low-frequency wing of the stationary profile at $\Omega \approx -15\gamma_1$.

Using calculations similar to those that led to the results shown in Fig. 4, one can determine the time of formation T_c of the stationary spectrum with the aid of various criteria. In particular, we tested three criteria. In the first, the spectrum was assumed to be steady, when as τ increased, starting from a specified value $\tau = T_c$, the oscillations of the maximum amplitude of the profile $\rho_1(\Omega_0, \tau)$, were less than 5% of the stationary value $\rho_1(\Omega_0, \infty) = \rho_{\max}$. In the second and third criteria, instead of the amplitude, the location of the centroid of the spectrum and the frequency Ω_0 of the profile maximum, respectively, were checked. The discrepancy of the T_c values, determined by three methods, was less than 30% with Ω_0 , Δ , V_1 , and q ranging between fairly wide limits. The calculated T_c values obtained with the use of the last criterion are given in Table I as a function of Ω_0 for the case $A_2 / A_1 - V_2^2 / V_1^2 = 0.01$, $V_2 = \gamma_1$. The value of Δ was determined from Eq. (2a) on the basis of the given values of Ω_0 , V_2 , and q . Table I also shows the corresponding calculated values of the halfwidth Γ of the stationary profile and its maximum amplitude ρ_{\max} . We note the rapid increase of $T_c \propto \Omega_0^2 / \gamma_1^3$ as Ω_0 increases and the proportionality $\rho_{\max} \propto 1/T_c$ at large T_c . Additional calculations show that doubling the value of V_2 results in a threefold uniform decrease of T_c relative to $|\Omega_0|$. In the case $A_1 = A_2$ for $V_1 = 10\gamma_1$, $V_2 = \gamma_1$, the values of T_c are one to two orders of magnitude smaller than the corresponding times given in Table I. The ratio of the initial level populations has little effect on T_c .

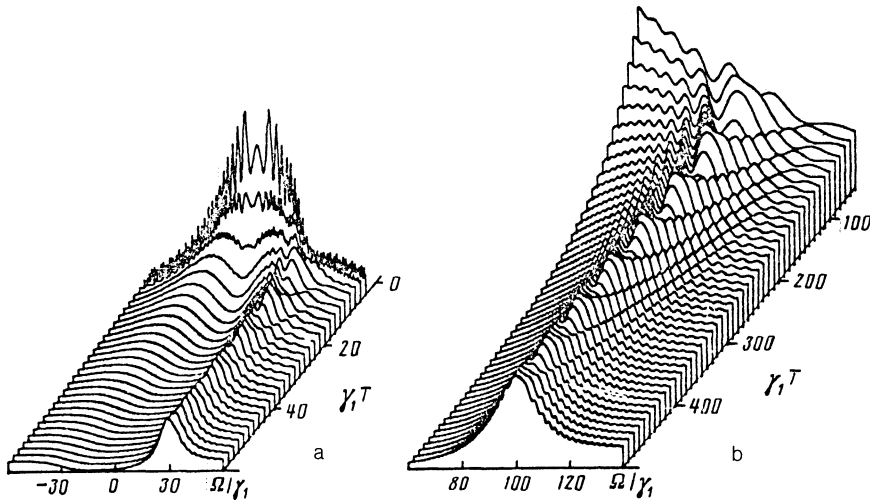


FIG. 4. Dynamics of formation of the stationary profile: $\Delta = 3\gamma_1$ (a), $0.98\gamma_1$ (b); $A_1 = A_2$, $V_1 = 10\gamma_1$, $V_2 = \gamma_1$, $\rho_0(0) = 0.7$, $\rho_2(0) = 0.3$; $\gamma = \Gamma_3 = 0$, $\Gamma_1 = \Gamma_2 = \gamma_1/2$.

On the basis of the data of Table I, we estimate the maximum value of the attainable interference shift. We set $T_c \sim \tau_{\text{coh}} \sim 1/\delta\nu$, where τ_{coh} is the time during which the field-induced coherence on the low-frequency transition of the atom is maintained, and $\delta\nu$ is the frequency range specifying the degree of nonmonochromaticity of laser radiation of frequency $\nu = \omega/2\pi$. The ratio $\delta\nu/\nu$ for stabilized laser sources can reach 10^{-13} – 10^{-14} (Ref. 21), which for $\gamma_1 = 10^8 \text{ sec}^{-1}$ and $\nu \sim 10^{15} \text{ sec}^{-1}$ yields the estimate $T_c \gamma_1 \sim 10^6$ – 10^7 . As follows from Table I, the interference shift Ω_0 for such values of $T_c \gamma_1$ amounts to over a thousand linewidths γ_1 of the allowed transitions. The splitting Δ required for the formation of this shift is either very small, $\Delta \approx 0.05\gamma_1$ ($\Omega_0 > 0$), or, on the contrary, large: $\Delta \approx 2000\gamma_1$ ($\Omega_0 < 0$). The power of spontaneous emission from the upper level $\sim \gamma_1 \rho_{\text{max}} h\nu n$ at an atomic density $n \sim 10^{12} \text{ cm}^{-3}$ and $\rho_{\text{max}} \approx 1.5 \times 10^{-5}$ is $\sim 1 \text{ mW}$, which is completely sufficient for reliable experimental measurement of a giant interference shift. The feasibility of such a measurement is also indicated by the fact that the recording of "nonabsorption resonances,"^{10–12} which have the same physical nature as the shift in question, was carried out with the aid of a multimode dye laser not stabilized in frequency. This may indicate that the ratio $\tau_{\text{coh}} \gg 1/\delta\nu$ actually holds, which facilitates observation of a giant shift.

Fairly stringent limitations on the technical parameters of the experiment setup are imposed by the transit effects.

TABLE I. Time of formation T_c of stationary spectrum vs location Ω_0 of line center.

Ω_0/γ_1	Δ/γ_1	Γ/γ_1	ρ_{max}	$T_c \gamma_1$
1	9,0	$1,3 \cdot 10^1$	$3,0 \cdot 10^{-1}$	$2,2 \cdot 10^1$
10	4,1	$2,3 \cdot 10^1$	$9,8 \cdot 10^{-2}$	$2,0 \cdot 10^2$
10^2	$4,9 \cdot 10^{-1}$	$1,8 \cdot 10^2$	$1,6 \cdot 10^{-3}$	$1,0 \cdot 10^4$
10^3	$5,0 \cdot 10^{-2}$	$1,8 \cdot 10^3$	$1,6 \cdot 10^{-5}$	$1,0 \cdot 10^6$
-1	1,1	$1,2 \cdot 10^1$	$3,5 \cdot 10^{-1}$	$1,6 \cdot 10^1$
-10	$2,4 \cdot 10^1$	$1,5 \cdot 10^1$	$2,4 \cdot 10^{-1}$	$1,9 \cdot 10^2$
-10^2	$2,0 \cdot 10^2$	$1,0 \cdot 10^2$	$5,0 \cdot 10^{-3}$	$1,7 \cdot 10^4$
-10^3	$2,0 \cdot 10^3$	$1,0 \cdot 10^3$	$5,0 \cdot 10^{-5}$	$1,6 \cdot 10^6$

Indeed, when the diameter of the light beam is 10 cm, and the velocity of the atoms, $\sim 10^4 \text{ cm/sec}$, the time of flight of the atoms through the light beam in the absence of collisions is $\tau_{\text{fl}} \sim 10^{-4} \text{ sec}$, which is two orders of magnitude smaller than the T_c corresponding to a shift of $\sim 10^3 \gamma_1$, and makes it possible to record shifts of $\sim 10^2 \gamma_1$. Therefore, observation of larger shifts requires special steps to increase τ_{fl} , for example, the use of an atomic beam intersecting the light beam at a small angle, the introduction of a low-pressure buffer gas into the volume studied, or a complete filling of the cell by a beam of radiation with the use of a wall coating such that the atoms are only slightly perturbed when they collide with it.

4. LINE PROFILE OF STATIONARY ABSORPTION IN THE PRESENCE OF COLLISIONS

The exact solution of the system of equations (1) in the stationary case for $\gamma, \Gamma_3 \neq 0$ is

$$\rho_1(\Omega) = \frac{[2V_1^2 V_2^2 + \gamma(V_2^2 G_1 + V_1^2 G_2 - 2V_1^2 V_2^2 Q)]}{[6V_1^2 V_2^2 + (A_1 + 3\gamma)V_2^2 G_1 + (A_2 + 3\gamma)V_1^2 G_2 + (\gamma_1 - 6\gamma)V_1^2 V_2^2 Q + \gamma\gamma_1(G_1 G_2 - V_1^2 V_2^2 Q^2)]}, \quad (3)$$

$$G_{1,2} = \bar{\Gamma}_{1,2} + [\bar{\Gamma}_{2,1} \bar{\Omega}_{1,2}^2 + V_1^2 V_2^2 D'' (\bar{\Gamma}_{1,2} D'' \mp 2\bar{\Omega}_{1,2} D')]/\text{Det},$$

$$Q = D' + [\bar{\Omega}_1 \bar{\Omega}_2 D' - (\bar{\Gamma}_1 \bar{\Omega}_2 - \bar{\Gamma}_2 \bar{\Omega}_1) D'' - V_1^2 V_2^2 D' D''^2]/\text{Det},$$

$$\text{Det} = \bar{\Gamma}_1 \bar{\Gamma}_2 - V_1^2 V_2^2 D'^2, \quad D' = \Gamma_3 / (\Gamma_3^2 + \Delta^2), \quad D'' = \Delta / (\Gamma_3^2 + \Delta^2),$$

$$\bar{\Gamma}_1 = \Gamma_1 + V_2^2 D', \quad \bar{\Gamma}_2 = \Gamma_2 + V_1^2 D',$$

$$\bar{\Omega}_1 = \Omega + V_2^2 D'', \quad \bar{\Omega}_2 = \Omega + \Delta - V_1^2 D''.$$

The numerator and denominator of the expression (3) for $\rho_1(\Omega)$ are, respectively, polynomials of the second and fourth degrees in Ω , and therefore, $\rho_1(\Omega)$ may be represented as a sum of a Lorentzian profile and its product by a dispersive profile with a shifted center. When the pressure tends to zero, the first of these profiles changes into the expression (2), and the second completely disappears. A more detailed analysis of (3) involving expansion of the quantities entering into $\rho_1(\Omega)$ in various limiting cases is very involved, and we shall confine ourselves to a numerical construction of the complete profile in cases (a) $A_2/A_1 = V_2^2/V_1^2 = 0.01$ (Fig. 5a) and (b) $A_1 = A_2$, $V_2 = 0.1 V_1 = \gamma_1$ (Fig. 5b), assuming for specificity the following de-

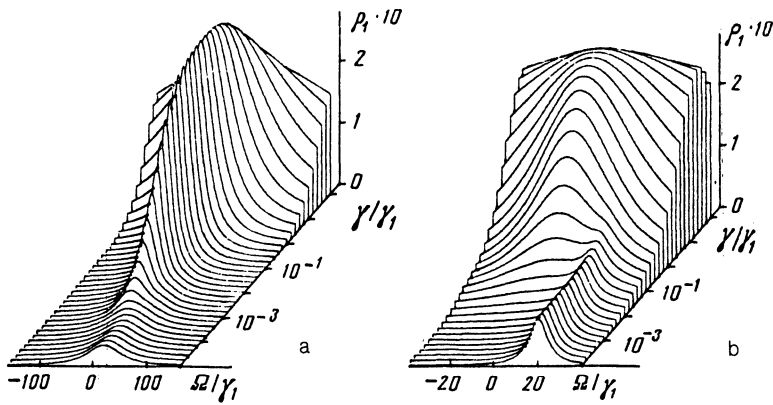


FIG. 5. Line profile as a function of gas pressure: (a) $A_2/A_1 = V_2^2/V_1^2 = 0.01$, $V_1 = 10 \gamma_1$, $\Delta = 2.34 \gamma_1$, (b) $A_1 = A_2$, $V_1 = 10 \gamma_1$, $V_2 = \gamma_1$, $\Delta = 4.11 \gamma_1$.

pendence of the quantities Γ_1 , Γ_2 , and Γ_3 on the gas pressure p : $\Gamma_1 = \Gamma_2 = \gamma_1/2 + 1.5\gamma$, $\Gamma_3 = 1.5\gamma$, $\gamma \propto p$. It is evident from Fig. 5 that the transformation of the complete profile as the pressure changes clearly reveals its components. However, the nature of the superposition of the profiles in cases (a) and (b) is qualitatively different: while in the second case, as γ increases, there is a simple superposition of components having different widths and centers, in the first case the two components are combined into a single Lorentzian profile with for which the width and position of the maximum vary continuously.

Highly indicative of the role of collisions in the presence of interference effects is Fig. 6, which shows the quantities Ω_0 , Γ , and ρ_{\max} , for the profiles given in Fig. 5, as functions of γ/γ_1 . It is evident from Fig. 6a that, starting with the

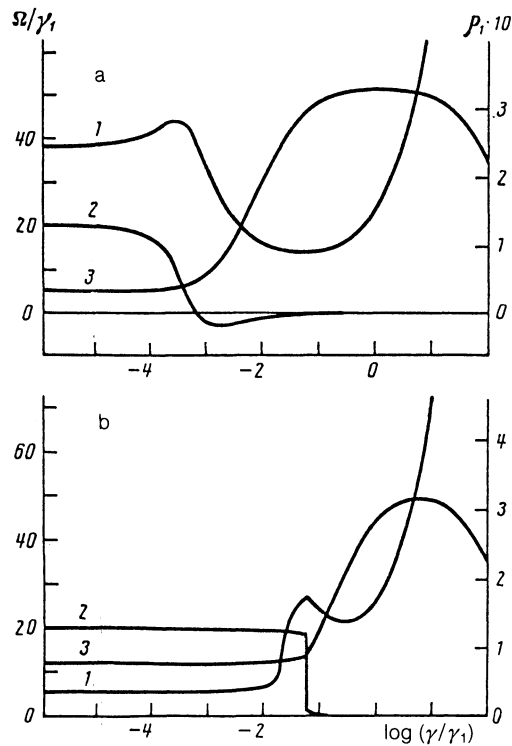


FIG. 6. Halfwidth Γ (curves 1), location Ω_0 of center (2), and size of the maximum ρ_{\max} (3) of the profiles shown in Fig. 5a (a), 5b (b) as a function of pressure. The values of Γ and Ω_0 are plotted along the ordinate on the left, and ρ_{\max} , on the right.

values $\gamma \sim 10^{-4} \gamma_1$, as the pressure increases, the collisions actively affect the formation of the line profile. The large interference shift decreases until its sign changes, and there is a simultaneous decrease of the profile width as its maximum increases. Starting with $\gamma/\gamma_1 \sim 0.1-1$, increasing the pressure depresses the NIE further. Thus, in the case discussed, collisions exert an influence on the profile that is analogous to that involved in spectral exchange.¹⁴⁻¹⁷ This fact is explained by the manifestation of the real component of the coupling parameter of the polarizations R_1 and R_2 when $\Gamma_3 \neq 0$ [see Eqs. (1')] and also by the fact that the narrowing of the line as the pressure increases as a result of "purely collisional" spectral exchange takes place in the presence of a real coupling coefficient.

More destructive is the role of collisions in case (b), where it is altogether impossible to talk about a narrowing of the profile as the pressure increases, despite a certain decrease of its width (Fig. 6b), since such characteristics as Ω_0 , Γ , and ρ_{\max} do not fully characterize the complex composite profile $\rho_1(\Omega)$.

We shall estimate the range of pressures in which collisional narrowing takes place in case (a). Assuming $\gamma = \gamma_0 p$, $\gamma_0 \approx 30$ MHz/torr, $\gamma_1 = 10^8$ sec⁻¹, and extracting from Fig. 6a the relation $3 \times 10^{-3} \lesssim \gamma/\gamma_1 \lesssim 1$, we obtain 0.3×10^{-2} torr $\lesssim p \lesssim 3$ torr, i.e., a range of sufficiently high pressures for cell measurements to be carried out.

5. OTHER CONFIGURATIONS OF A CLOSED THREE-LEVEL SYSTEM

We shall discuss the qualitative manifestations of NIE in closed three-level systems of other possible types: when the upper state is split, and with a quasi-equidistant arrangement of the levels forming two successive transitions. The fundamental difference between these systems and that discussed above is that level 2 is no longer metastable, so that the polarization R_3 induced by the field on the forbidden transition 0-2, even in the absence of collisions, will have a time lag due to the spontaneous decay of the upper states: $\Gamma_3 = (A_1 + A_2)/2$. This factor will obviously mask the large interference shift of the stationary absorption line. The question lies in the degree and character of suppression of the effect. We shall examine it in more detail, using the example of a system with close excited levels 1 and 2 and ground state 0.

The initial system of equations for this case, keeping the previous notation, is

$$\begin{aligned}
\dot{R}_1 + (\Gamma_1 - i\Omega)R_1 &= iV_1(\rho_0 - \rho_1) - iV_2R_3^*, \\
\dot{R}_2 + [\Gamma_2 - i(\Omega + \Delta)]R_2 &= iV_2(\rho_0 - \rho_2) - iV_1R_3, \\
\dot{R}_3 + (\Gamma_3 - i\Delta)R_3 &= iV_2R_1^* - iV_1R_2, \\
\dot{\rho}_0 - A_1\rho_1 - A_2\rho_2 &= 2V_1 \operatorname{Re} iR_1 + 2V_2 \operatorname{Re} iR_2, \\
\dot{\rho}_2 + A_1\rho_1 + \gamma(\rho_1 - \rho_2) &= -2V_1 \operatorname{Re} iR_1, \\
\rho_0 + \rho_1 + \rho_2 &= 1.
\end{aligned} \tag{4}$$

The following expression results from Eqs. (4) for the stationary energy of the field:

$$\begin{aligned}
\mathcal{P} = & -2[2\gamma_1 V_1^2 V_2^2 + (A_1 A_2 + \gamma\gamma_1)(V_2^2 G_1 + V_1^2 G_2 - 2V_1^2 V_2^2 Q)] / \\
& [12V_1^2 V_2^2 + 2(2A_1 + 3\gamma)V_2^2 G_1 + 2(2A_2 + 3\gamma)V_1^2 G_2 \\
& - 2(\gamma_1 + 6\gamma)V_1^2 V_2^2 Q + (A_1 A_2 + \gamma\gamma_1)(G_1 G_2 - V_1^2 V_2^2 Q^2)]. \tag{5}
\end{aligned}$$

The notation entering into Eq. (5) is the same as in Eq. (3), with the exception of the change of sign of Δ .

It is evident from Eq. (5) that its structure, which determines the dependence of the profile on Ω , V_1 , and V_2 , is completely identical to Eq. (3). Setting $\gamma = 0$ in Eq. (5), we can identify the quantity γ entering into Eq. (3) with the product $A_1 A_2 / \gamma_1$. As a result, the numerators of Eqs. (3) and (5) are the same, and the denominators are different only in the numerical coefficients, or in the frequency-independent multipliers of the individual terms. Thus, the general considerations of the profile structure cited in the discussion of Eq. (3) remain in force. However, since the collisional relaxation time γ^{-1} , which determines the transformation of the line profile as the pressure changes, in this case is replaced by the sum of the irradiation times $A_1^{-1} + A_2^{-1}$, the complete profile (5) contains two components also in the absence of collisions, which prevents one from distinguishing an interference profile with a large shift.

Numerical calculations of $\mathcal{P}(\Omega)$ (5), analogous to those that produced the results presented in Fig. 5, showed that in the absence of collisions in the case $A_1 = A_2$ (b), the interference profile is approximately an order of magnitude narrower than the noninterference profile, and as Δ increases, shifts from the initial position to the left of the center of the latter (within a halfwidth), when $\Delta = 0$ to appreciable distances $\sim \Delta$ at large Δ . This is associated with an increasingly distinct separation of the interference profile without any appreciable change in width and in maximum amplitude.

Increasing the interaction with the field while the ratio V_2/V_1 remains constant increases the amplitude and decreases the width of the interference component relative to the noninterference component. In the case of $A_1 \neq A_2$ (a), the two components of the complete profile have approximately the same widths and amplitudes and are therefore difficult to separate. When Δ changes, the presence of the interference part of the profile can only be determined from a certain "waviness" of the right-hand wing of $\mathcal{P}(\Omega)$, transformed into a small maximum near $\Omega \approx \Delta$, when Δ exceeds the profile width. Thus, in both cases, the NIE also manifest

themselves quite clearly in a three-level system with close upper levels, but not in pure form such as the formation of a giant line shift when the splitting of the ground state tends to zero.

6. CONCLUSION

These interference effects may be of practical interest in a precise determination of the frequencies and wavelengths of resonance transitions of atoms and molecules with frozen rotational degrees of freedom. In particular, they should be considered among the factors limiting the stability and reproducibility of laser standards of wavelength. The extreme behavior of the shift associated with a decrease in the splitting of the sublevels of the ground state offers possibilities for studying the statistical properties of laser radiation and radiation of collisional and radiation relaxation between the components of the splitting.

¹The magnetic-dipole and quadrupole-radiative transition times between the sublevels of split atomic ground states amount to ≈ 1 sec,¹³ which is much greater than the characteristic times of the problem, 10^{-8} sec, determined by the relaxation constants of the levels and by the probability of stimulated radiative transitions under saturation conditions.

²Here and below, the radiation pulse was assumed rectangular in numerical calculations of the time dependences.

¹M. S. Zubova and V. P. Kochanov, *Pis'ma Zh. Eksp. Teor. Fiz.* **50**, 376 (1989) [*JETP Lett.* **50**, 406 (1989)].

²S. G. Rautian, G. I. Smirnov, and A. M. Shalagin, *Nonlinear Resonances in Atomic and Molecular Spectra* (Nauka, Novosibirsk, 1979) [in Russian].

³I. M. Beterov and R. I. Sokolovskii, *Usp. Fiz. Nauk* **110**, 169 (1973).

⁴*Laser Spectroscopy of Atoms and Molecules*, edited by H. Walther (Springer, New York, 1976).

⁵N. Blombergen, *Nonlinear Spectroscopy* (Benjamin, New York, 1965).

⁶G. E. Notkin, S. G. Rautian, and A. A. Feoktistov, *Zh. Eksp. Teor. Fiz.* **52**, 1673 (1967) [*Sov. Phys. JETP* **25**, 1112 (1967)].

⁷R. I. Sokolovskii, *Opt. Spektrosk.* **27**, 1017 (1969) [*Opt. Spectrosc. (USSR)* **27**, 553 (1969)].

⁸Im Thek-de, S. G. Rautian, E. G. Saprykin *et al.*, *Zh. Eksp. Teor. Fiz.* **62**, 1661 (1972) [*Sov. Phys. JETP* **35**, 865 (1972)].

⁹S. G. Rautian and Ya. S. Bobovich, *Opt. Spektrosk.* **34**, 617 (1973) [*Opt. Spectrosc. (USSR)* **34**, 356 (1973)].

¹⁰G. Alzetta, A. Gozzini, and G. Orriols, *Nuovo Cimento* **36B**, 5 (1976).

¹¹G. Alzetta, L. Moi, and G. Orriols, *Nuovo Cimento* **52B**, 209 (1979).

¹²G. Orriols, *Nuovo Cimento* **53B**, 1 (1979).

¹³H. Bethe and E. Salpeter, *Quantum Mechanics of One- and Two-Electron Systems* (Springer, Berlin, 1958).

¹⁴M. Baranger, *Phys. Rev.* **111**, 481 (1958).

¹⁵A. C. Kolb and H. Griem, *Phys. Rev.* **111**, 514 (1958).

¹⁶V. Fano, *Phys. Rev.* **131**, 259 (1963).

¹⁷A. I. Burshtein, *Lectures in a Course of Quantum Kinetics, Part II* (NGU, Novosibirsk, 1968) [in Russian].

¹⁸V. S. Butylkin, A. E. Kaplan, Yu. G. Khronopolu, and E. I. Yakubovich, *Resonant Nonlinear Interactions of Light With Matter* (Springer, New York, 1989).

¹⁹I. I. Sobel'man, *Introduction to the Theory of Atomic Spectra* (Pergamon, Oxford, 1973).

²⁰R. Karplus and I. A. Schwinger, *Phys. Rev.* **73**, 1020 (1948).

²¹S. N. Bagaev, E. V. Baklanov, and V. P. Chebotayev, *Pis'ma Zh. Eksp. Teor. Fiz.* **16**, 344 (1972) [*JETP Lett.* **16**, 243 (1972)].

Translated by Adam Peiperl